



VICTORIA UNIVERSITY
MELBOURNE AUSTRALIA

Improving expansive clay subgrades using recycled glass: Resilient modulus characteristics and pavement performance

This is the Accepted version of the following publication

Yaghoubi, Ehsan, Yaghoubi, Mohammadjavad, Guerrieri, Maurice and Sudarsanan, N (2021) Improving expansive clay subgrades using recycled glass: Resilient modulus characteristics and pavement performance. *Construction and Building Materials*, 302. ISSN 0950-0618

The publisher's official version can be found at
<https://www.sciencedirect.com/science/article/pii/S0950061821021425?via%3Dihub>
Note that access to this version may require subscription.

Downloaded from VU Research Repository <https://vuir.vu.edu.au/42492/>

1 1 Improving expansive clay subgrades using recycled glass: Resilient
2 2 modulus characteristics and pavement performance
3
4

5 3
6 4
7 5 Ehsan Yaghoubi, BSc, MSc, PhD*
8 6 College of Engineering & Science, Victoria University, Melbourne, Australia
9 7 E-mail: ehsan.yaghoubi@vu.edu.au
10 7

11 8
12 9 Mohammadjavad Yaghoubi, BSc, MEngSc, PhD
13 10 Australian Road Research Board, Melbourne, Australia, &
14 11 Hydrogeological Engineering Research Group (GHERG), Federation University Australia,
15 11 Churchill, Australia
16 12 E-mail: Javad.Yaghoubi@arrb.com.au
17 13
18 14

19 15 Maurice Guerrieri, BEng, PhD
20 16 Institute for Sustainable Industries and Liveable Cities, Victoria University, Melbourne,
21 16 Australia
22 17 E-mail: maurice.guerrieri@vu.edu.au
23 18
24 19

25 20 Nithin Sudarsanan, PhD
26 21 Department of Civil, Construction, and Environmental Engineering, North Carolina State
27 21 University, Raleigh, USA.
28 22 E-mail: nsudars@ncsu.edu
29 23
30 24

31 25 * Corresponding Author:
32 26 Ehsan Yaghoubi
33 27 Lecturer, College of Engineering & Science, Victoria University
34 27 Room D304, Level 3, Building D, Victoria University, Victoria 3011 Australia
35 28 E-mail: ehsan.yaghoubi@vu.edu.au
36 29 Telephone: +61 3 9919 4804
37 30
38 31
39
40
41
42
43
44
45
46
47
48
49
50
51
52
53
54
55
56
57
58
59
60
61
62
63
64
65

Improving expansive clay subgrades using recycled glass: Resilient modulus characteristics and pavement performance

Abstract

The scarcity of sound soils, especially in urban areas, often forces engineers to construct the pavement on problematic subgrade soils such as expansive clays. The associated cost involved in replacing the existing problematic soil is avoided by adopting treatment techniques. In this study, a type of high plasticity expansive clay was mixed with 10, 20, and 30% sand-size recycled glass (RG) as a non-chemical soil treatment approach. An extensive investigation comprising experimental works, numerical modeling, and pavement performance analysis was undertaken. After determination of the physical properties of clay and RG, resilient modulus characteristics of clay and the three clay-RG mixtures were carried out through an experimental program. Subsequently, the obtained resilient modulus data sets were incorporated into a finite element analysis program in order to analyze the stress-strain response of pavement models founded on clay and RG-treated subgrades. The compressive and tensile strains achieved through the analysis of the pavement models under traffic loads were next used to compare each pavement model with respect to fatigue and rutting performances. The experimental results showed up to a 113% increase in resilient modulus of clay by the addition of 30% RG. The outcomes of the analysis on pavement systems modeled using the experimental input showed a considerable reduction in compressive and tensile strains by treating the clay subgrade with RG. Consequently, the strain reduction exhibited a significant increase in fatigue life and rutting life of pavements founded on RG treated clay subgrades. The outcomes of this research aim to encourage the construction industry to consider the utilization of environmentally clean recycled aggregates, such as RG, for improving subgrades with problematic soils and hence, promote sustainable construction materials and approaches.

Keywords: Recycled glass, expansive clay, subgrade treatment, pavement response analysis, rutting and fatigue life

1 Introduction

The urbanization, industrialization, and the consequent dramatic population increase, especially in metropolitan areas, have led to considerable growth in construction activities. Transportation infrastructure projects, especially those related to pavements of roads, are a continuous construction activity in urban areas to meet the transport needs of the growing population. The typical structure of flexible pavements comprises an asphalt concrete surface course, unbound granular base (and an optional subbase) course with the subgrade soil as the foundation. In urban areas, due to space limitations and hence, dictated road alignments, pavements may need to be constructed on problematic subgrades, such as expansive clay soils. Expansive soils are typically rich in hydrophilic minerals such as illite and montmorillonite, making them significantly sensitive to moisture changes. Expansive clays swell (increase in volume) as a result of increased moisture content and shrink (decrease in volume) due to drying. This behavior of expansive soils as a road subgrade results in heave, subsidence, and uneven road surfaces, which lead to several types of pavement distresses, such as the emergence of cracks on the surface of the road and premature deterioration [1, 2].

1 1 Improving expansive clay subgrades using recycled glass: Resilient
2 2 modulus characteristics and pavement performance
3
4

5 3
6 4
7 5 Ehsan Yaghoubi, BSc, MSc, PhD*
8 6 College of Engineering & Science, Victoria University, Melbourne, Australia
9 7 E-mail: ehsan.yaghoubi@vu.edu.au
10 7

11 8
12 9 Mohammadjavad Yaghoubi, BSc, MEngSc, PhD
13 10 Australian Road Research Board, Melbourne, Australia, &
14 11 Hydrogeological Engineering Research Group (GHERG), Federation University Australia,
15 11 Churchill, Australia
16 12 E-mail: Javad.Yaghoubi@arrb.com.au
17 13
18 14

19 15 Maurice Guerrieri, BEng, PhD
20 16 Institute for Sustainable Industries and Liveable Cities, Victoria University, Melbourne,
21 16 Australia
22 17 E-mail: maurice.guerrieri@vu.edu.au
23 18
24 19

25 20 Nithin Sudarsanan, PhD
26 21 Department of Civil, Construction, and Environmental Engineering, North Carolina State
27 21 University, Raleigh, USA.
28 22 E-mail: nsudars@ncsu.edu
29 23
30 24

31 25 * Corresponding Author:
32 26 Ehsan Yaghoubi
33 27 Lecturer, College of Engineering & Science, Victoria University
34 27 Room D304, Level 3, Building D, Victoria University, Victoria 3011 Australia
35 28 E-mail: ehsan.yaghoubi@vu.edu.au
36 29 Telephone: +61 3 9919 4804
37 30
38 31
39
40
41
42
43
44
45
46
47
48
49
50
51
52
53
54
55
56
57
58
59
60
61
62
63
64
65

32 Improving expansive clay subgrades using recycled glass: Resilient 33 modulus characteristics and pavement performance

35 Abstract

36 The scarcity of sound soils, especially in urban areas, often forces engineers to construct the
37 pavement on problematic subgrade soils such as expansive clays. The associated cost
38 involved in replacing the existing problematic soil is avoided by adopting treatment
39 techniques. In this study, a type of high plasticity expansive clay was mixed with 10, 20, and
40 30% sand-size recycled glass (RG) as a non-chemical soil treatment approach. An extensive
41 investigation comprising experimental works, numerical modeling, and pavement
42 performance analysis was undertaken. After determination of the physical properties of clay
43 and RG, resilient modulus characteristics of clay and the three clay-RG mixtures were
44 carried out through an experimental program. Subsequently, the obtained resilient modulus
45 data sets were incorporated into a finite element analysis program in order to analyze the
46 stress-strain response of pavement models founded on clay and RG-treated subgrades. The
47 compressive and tensile strains achieved through the analysis of the pavement models
48 under traffic loads were next used to compare each pavement model with respect to fatigue
49 and rutting performances. The experimental results showed up to a 113% increase in
50 resilient modulus of clay by the addition of 30% RG. The outcomes of the analysis on
51 pavement systems modeled using the experimental input showed a considerable reduction
52 in compressive and tensile strains by treating the clay subgrade with RG. Consequently, the
53 strain reduction exhibited a significant increase in fatigue life and rutting life of pavements
54 founded on RG treated clay subgrades. The outcomes of this research aim to encourage the
55 construction industry to consider the utilization of environmentally clean recycled
56 aggregates, such as RG, for improving subgrades with problematic soils and hence, promote
57 sustainable construction materials and approaches.

59 **Keywords:** Recycled glass, expansive clay, subgrade treatment, pavement response
60 analysis, rutting and fatigue life

62 1 Introduction

63 The urbanization, industrialization, and the consequent dramatic population increase,
64 especially in metropolitan areas, have led to considerable growth in construction activities.
65 Transportation infrastructure projects, especially those related to pavements of roads, are a
66 continuous construction activity in urban areas to meet the transport needs of the growing
67 population. The typical structure of flexible pavements comprises an asphalt concrete
68 surface course, unbound granular base (and an optional subbase) course with the subgrade
69 soil as the foundation. In urban areas, due to space limitations and hence, dictated road
70 alignments, pavements may need to be constructed on problematic subgrades, such as
71 expansive clay soils. Expansive soils are typically rich in hydrophilic minerals such as illite
72 and montmorillonite, making them significantly sensitive to moisture changes. Expansive
73 clays swell (increase in volume) as a result of increased moisture content and shrink
74 (decrease in volume) due to drying. This behavior of expansive soils as a road subgrade
75 results in heave, subsidence, and uneven road surfaces, which lead to several types of
76 pavement distresses, such as the emergence of cracks on the surface of the road and
77 premature deterioration [1, 2].

78 Traditionally, to mitigate the significant potential for volume change in expansive clay,
1 79 chemical binders such as lime and cement have been used [2]. Several researchers have
2 80 made attempts to promote solid waste as alternative construction materials to the traditional
3 81 lime and cement treatment methods to mitigate the environmental and economic drawbacks.
4 82 The soil improvement by the utilization of solid wastes can be achieved by chemical and/or
5 83 non-chemical methods. Chemical stabilizers improve the properties of expansive clay
6 84 through chemical reactions, whereas with non-chemical stabilizers, the soil improvement is
7 85 achieved by reinforcing the soil structure. In recent years, various types of solid wastes have
8 86 been introduced and evaluated as chemical stabilizers, such as fly ash [3], calcium carbide
9 87 residue [4], lime kiln dust [5]. Several scholars have investigated the improvement of
10 88 subgrade soils using a combination of chemical and non-chemical stabilizers, such as spent
11 89 coffee and geopolymers [6], short polypropylene fibers and polyvinyl alcohol polymer [7], rice
12 90 husk ash and cement [8], polyethylene terephthalate fiber and fly ash [9]. Under non-
13 91 chemical stabilizing, researchers have mainly used various types of fibers, such as carpet
14 92 waste fibers [10], rubber fibers [11] polyester fibers [12]. However, the non-chemical
15 93 stabilization approach using sand-like particles, such as recycled glass, has been scarcely
16 94 investigated in the literature.

19
20 95 Recycled glass (RG) is a product of recycling industries and is broadly used in construction
21 96 projects as an individual sand-size construction material [13, 14] or in combination with other
22 97 natural or recycled aggregates [15, 16]. RG consists of various colored crushed glass
23 98 particles and often debris such as paper, plastic, and food waste, if not washed. Containing
24 99 glass particles with different colors is the main obstacle for RG to be re-used in bottle
25 100 production industries. This drawback, combined with the desirable engineering properties of
26 101 recycled glass, makes the construction industry a suitable destination for this material [14].
27 102 In Australia, the application of RG as a construction material is encouraged in practicing
28 103 construction guidelines, such as Austroad's Guide to Pavement Technology, Part 4 [17], and
29 104 Sewerage Standards for Embedment [18]. The environmental footprint of RG has been
30 105 investigated by several researchers [19, 20] who concluded that RG is an environmentally
31 106 clean material that complies with regulatory requirements such as EPA-Victoria [21] and
32 107 U.S.EPA [22].

35 108 Despite the early promise, comprehensive investigations on RG's true capacity to stabilize
36 109 subgrade soils have been very limited to date. Eberemu, et al. [23] mixed up to 20% of RG
37 110 with the maximum particle size of 4.75 mm with a type of lateritic clay and carried out
38 111 geotechnical tests on the mixtures. Their results showed up to a 15.5% reduction in plasticity
39 112 index, up to 44% increase in friction angle, and up to 70% increase in California Bearing
40 113 Ratio (CBR). Wartman, et al. [24] added up to 90% of two types of well-graded sand-size RG
41 114 to fine soils, which resulted in increased unit weight and improved shear strength
42 115 characteristics of the soils. Strength characteristics of cement stabilized expansive clay
43 116 mixed with up to 20% of fine recycled glass (< 300 μ m) were studied by Ikara, et al. [25].
44 117 Their results showed further increase in bearing capacity (CBR), and unconfined
45 118 compressive strength (UCS) of the cement stabilized expansive clay.

48
49 119 The few studies mentioned above that investigated the behavior of clay-RG mixtures mainly
50 120 focused on their basic geotechnical properties such as plasticity, CBR and UCS. The
51 121 evaluation of the response and performance of the subgrade through nearly static
52 122 experimental methods, such as CBR, do not satisfactorily simulate the behavior of a
53 123 pavement system that undergoes repeated loadings of vehicular traffic [26]. For a more
54 124 realistic evaluation of the performance and stress-strain response of pavement materials
55 125 under repeated loading, the resilient modulus (M_r) concept was introduced by Seed, et al.
56 126 [27], which accounts for the stiffness characteristics of pavement materials. Ever since,
57 127 pavement experts have repeatedly evaluated the performance of treated and untreated
58 128 subgrade soils using the resilient modulus characteristics commonly obtained by Repeated
59 129 Load Triaxial (RLT) testing. However, to the best of the authors' knowledge, no experimental

research has been carried out on the resilient properties of subgrade clays improved by the addition of sand-size recycled glass.

While several studies have focused on the experimental evaluation of treated subgrades, analysis of their resilient response in pavement systems using the experimental results is still lacking. In this research, an experimental program was used to evaluate the resilient modulus characteristics of clay-RG samples, followed by a numerical stress-strain response analysis. The Mechanistic-Empirical Pavement Design Guide (MEPDG) [28] strongly encourages the utilization of the resilient modulus obtained through RLT testing for design purposes. Experimentally obtained resilient moduli can be used to determine the model coefficients of the predictive constitutive resilient modulus models. These coefficients remain the same for a certain type of soil and are typically used as a direct or indirect input in the pavement design and analysis software packages as the Level 1 MEPDG input.

The stress-strain response analyses in this research were carried out through a three-dimensional viscoelastic finite element analysis program, FlexPAVE™. This computer program is capable of evaluating the pavement behavior under repeated loads of various moving vehicles, at various pavement temperatures under different subgrade conditions [29]. Several researchers have validated the response analyses of FlexPAVE™ through comparison with field observations [30, 31]. In this research, the RLT test results on clay-RG mixtures were incorporated in FlexPAVE™ analysis as input parameters. The compressive and tensile strains achieved through the analyses were next used for a fatigue and rutting performance comparison analysis of the pavements modeled over untreated clay subgrades and those over RG-treated subgrades. The review of the literature showed that the study on the stress distribution and associated strains due to traffic loads on treated or untreated subgrades has not been focused on as much as experimental studies.

The experimental results, stress-strain response analyses, and performance analyses of the RG-treated subgrade soils used in this research aim to promote the application of recycled materials to support the circular economy while achieving the improved performance of subgrade materials. The sand-size recycled glass can be an alternative to relatively costly and less environmentally-friendly traditional methods of soil stabilization in road construction projects.

2 Materials and Methods

2.1 Materials and basic properties

Materials used in this research included a natural expansive clay found in the majority of the western metropolitan area of Melbourne, Australia, and sand-size recycled glass, supplied by a commercial recycling facility in Melbourne, Australia. In addition, for numerical modeling purposes, a typical asphalt concrete (AC) and aggregate base course (ABC) commonly used in North Carolina, USA being "S9.5B", and "Belgrade", respectively, were used. While physical and mechanical properties of the clay and RG were determined through an experimental program, properties of S9.5B and Belgrade ABC were obtained from previous studies [32, 33].

For carrying out experiments on clay, first, lumps of clay collected from a depth of 0.2-0.8 m were left in the oven, set to 50 °C for four days to dry. Dry clay lumps were next crushed to 5 mm pieces using a laboratory-scale crusher and subsequently ground using a soil grinder. Figure 1 shows the dried lumps of clay, together with the crusher, and the grinder used for preparing clay samples.

175 For the determination of the particle size distribution of Clay, a wet sieving procedure was
 176 followed. Figure 2 shows the plasticity and physical properties of Clay and RG. Coefficient of
 177 Uniformity (C_u) of 6 ($C_u \geq 6$) and Coefficient of Curvature (C_c) of 1.1 ($1 \leq C_c \leq 3$) classifies RG
 178 as a well-graded sand (SW) according to the UCSC classification scheme. Based on the
 179 liquid limit (LL) and plastic limit (PL) values of clay, presented in Figure 2, and following the
 180 USCS classification scheme, the Clay is classified as high plasticity clay (CH), containing
 181 11.8% sand-size particles.

182 In order to quantitatively assess the expansiveness of the Clay, shrink-swell tests were
 183 carried out following the AS-1289.7.1.1 [34] procedure. This test includes two companion
 184 tests -shrinkage test and swelling test. In this research, using a 50 mm diameter thin-walled
 185 tube, three undisturbed core samples were obtained from a depth of 0.5 - 1 m for each
 186 shrinkage and swelling test.

187 Shrinkage samples were trimmed and observed to be free of defects and/or voids. Small
 188 pins were weighted and pushed into the core from the two ends to facilitate a consistent
 189 length measurement throughout the shrinkage process. The mass and dimensions of
 190 samples at the initial state, during the air-drying process, and after oven-drying at 105-110°C
 191 were taken. The maximum shrinkage strains (ϵ_{sh}) were then calculated based on the
 192 measured lengths. The swelling test is a simplified oedometer test in which the sample is
 193 mounted in a rigid stainless steel ring of approximately 20 mm height and a diameter of 45
 194 mm. In this test, the ring containing the sample was placed between porous stones and
 195 mounted in the cell of the test apparatus. The apparatus was equipped with dial gages to
 196 measure the swelling (or settlement). Initially, an overburden pressure of 5 kPa was applied
 197 for 5 minutes followed by a pressure of 25 kPa for 30 minutes and the initial settlement was
 198 recorded. Next, the sample was submerged with distilled water and readings were
 199 undertaken until less than 5% variation in the swelling was observed for a period of at least 3
 200 hours. The measured sample heights were used to determine the maximum swell strains
 201 (ϵ_{sw}). Shrink-Swell index (I_{ss}) was next determined using Equation 1.

$$I_{SS} = \frac{\epsilon_{sh} + \frac{\epsilon_{sw}}{2}}{1.8} \quad (1)$$

203 Shrink-Swell index (I_{ss}) can be used for estimation of instability index which is the product of
 204 the lateral restrained factor, α , and I_{ss} [35]. Utilizing the instability index, the characteristic
 205 surface movement (y_s) can be determined for one type of soil layer using Equation 2
 206 adopted from AS-2870 [36].

$$y_s = \frac{I_{pt} \times \Delta\psi \times h}{100} \quad (2)$$

208 Where y_s is characteristic surface movement (mm), $\Delta\psi$ is the change in suction (taken 1.2
 209 pF as recommended by AS-2870 [36]), and h is the thickness of the soil layer (taken 1 m for
 210 subgrade). For the Clay used in this research, the average ϵ_{sh} , ϵ_{sw} and I_{ss} were 11.26, 2.18
 211 and 6.86, with standard deviations of 0.59, 0.20 and 0.38, respectively. Based on the I_{ss}
 212 value of 6.86 and considering the α factor of 1 (considering cracked zone near the surface of
 213 the subgrade) the value of y_s is determined to be 82.3 mm and hence, the construction site
 214 covered by such clay is classified as "extremely reactive" based on AS-2870 [36].

215 In this research, in order to investigate the improvement of resilient modulus characteristics
 216 of Clay using recycled glass, three mixtures of clay-glass (CG) with gravimetric RG contents
 217 of 10% (CG10), 20% (CG20) and 30% (CG30) were prepared to be compared with Clay
 218 samples as the benchmark.

2.2 Compaction and repeated load triaxial testing

The characterization of pavement subgrades in terms of resilient modulus (M_r) is strongly encouraged in the design of new pavements [28]. Values of M_r are typically obtained through repeated load triaxial (RLT) testing on undisturbed or reconstituted cylindrical specimens. In this research, RLT testing was carried out following the AASHTO-T307-99 [37] procedure to simulate repeated traffic loadings on pavements. A vehicle wheel traveling on a pavement structure is known to generate a stress pulse comprising of deviator and confining stress components [38]. Following the AASHTO-T307-99 [37] procedure, a haversine-shaped loading pulse with a loading period of 0.1s and a resting period of 0.9 s was applied. The confining stress and deviator stress for subgrade materials in AASHTO-T307-99 [37] range from 13.8 to 41.4 kPa and from 13.8 to 68.9 kPa, respectively. Table 1 presents the confining stress-bulk stress combinations applied in each loading sequence. Sequence No. 0 was the conditioning sequence and included 1000 load repetitions. The test continued with 15 sequences of 100 load repetitions each. The M_r value in each sequence (load combination) is the average of the M_r values achieved in the last 5 load repetitions.

For specimen preparation, clay and RG were initially mixed at the dry state to obtain homogenous 2 kg mixtures. The proportion of the two materials in the mixture was determined by calculating the amount of clay and RG using gravimetric contents as explained in the previous section. For instance, for preparing CG20 samples, 400 g of RG was mixed with 1600 g of clay to form a 2 kg dry sample. Next, the required amount of water, calculated based on the dry mass of the dry sample and the OMC, as presented in Figure 4, was measured and added. The mixtures were blended in a mechanical mixer for 3 minutes to ensure water was thoroughly mixed. The blends were then stored in containers sealed with plastic films for at least 48 hours to cure. Cylindrical RLT specimens were prepared at the optimum moisture content (OMC) and targeting Maximum Dry Density (MDD) achieved under a standard effort of 600 kN-m/m³ [39]. Based on AASHTO-T307-99 [37], the diameter of the RLT sample should be greater than 5 times the maximum particle size of the specimen. Given the maximum particle size of 4.75 mm in samples, a split mold with a diameter of 50 mm and a height of 100 mm was used for sample preparation. The materials were compacted in the steel cylindrical mold using an electric vibratory hammer, capable of 3000 blows per minute as specified by AASHTO-T307-99 [37], in four layers to achieve the required density. After compaction, specimens were carefully removed from the split mold, and to avoid moisture loss; they were quickly placed on the triaxial cell pedestal. Next, the rubber membrane was placed over the sample and was sealed to the pedestal and the top loading cap with a set of O-rings as recommended by AASHTO-T307-99 [37].

A total of 15 datasets of M_r - σ_c - θ were obtained through RLT testing on each of the four samples. These data sets were used to determine the model coefficients (k) of two commonly used constitutive M_r predictive models through regression analysis. The k parameters remain the same for a certain type of soil. The models used in this research included the two-parameter (also known as bulk stress) model proposed by Hicks and Monismith [40] and the modified universal model recommended by AASHTO [41] as presented in Equation 3 and Equation 4, respectively. Both models are used for fine and granular soils and the universal model is used in the MEPDG design procedure [28].

$$M_r = k_1 \cdot \theta^{k_2} \quad (3)$$

$$M_r = k_1 \cdot p_a \cdot \left(\frac{\theta}{p_a}\right)^{k_2} \cdot \left(\frac{\tau_{oct}}{p_a} + 1\right)^{k_3} \quad (4)$$

In these equations, k_1 to k_3 are regression parameters, p_a is the normalizing pressure which is equal to atmospheric pressure, θ is the bulk stress, which is the sum of vertical and

267 horizontal stresses, and τ_{oct} is the octahedral shear stress ($\frac{\sqrt{2}}{3}\sigma_d$, where σ_d is the deviator
268 stress).

269 **2.3 Numerical modeling for stress-strain response analysis**

270 In this research, modeling of the pavement structure and pavement response analysis was
271 carried out using the FlexPAVE™ program. Figure 3 shows the pavement profile that was
272 assigned to the model for stress-strain response analysis. The modeled profile is a typical
273 North Carolina pavement profile that is used for roads with less than 3 million equivalent
274 single axle loads (ESALs) [32]. The profile comprised of a 10.16 cm of asphalt concrete (AC)
275 layer, over a 15.24 cm layer of aggregate base course (ABC) which was over subgrade
276 layers. The pavement profile was analyzed under a 40 kN wheel load that is one of the pair
277 of wheels in the 80 kN single axle load moving at a speed of 80 km/h with a pavement
278 temperature of 23°C.

279 In the modeled profile, a typical AC type, being S9.5B was used for the surface course. The
280 S9.5B AC is a hot mix asphalt made of PG 58-28 asphalt with a nominal maximum
281 aggregate size of 9.5 mm, and contains 40% of reclaimed asphalt pavement. The stiffness
282 properties of S9.5B are presented in Table 2 in terms of Prony coefficients (ρ_i) extracted
283 from Cho [32]. Prony coefficients are input parameters in FlexPAVE™ and represent the
284 viscoelastic properties of AC. Prony coefficients are obtained by fitting results of dynamic
285 modulus testing [42] at various load frequencies and temperatures to the generalized
286 Maxwell model [32]. A typical quarry material, named "Belgrade" was defined as ABC with
287 the average measured Mr value of 101 kPa following AASHTO-T307-99 [37] procedure and
288 Poisson's Ratio of 0.4 adopted from the report by Chow, et al. [33]. Using RLT test results of
289 Chow, et al. [33] fitted to the Universal Model (Equation 4), k_1 , k_2 , and k_3 parameters for
290 Belgrade ABC were obtained as 0.863, 0.640, and 0.202, respectively. These parameters
291 can be used for the estimation of Mr values under the loading conditions presented in Figure
292 3.

293 Typically, although a minimum depth of 25 cm has been specified for stabilizing the
294 subgrade, the recommended depth is 30 cm [43]. As such, in the models developed in
295 FlexPAVE™, the top 30 cm of the subgrade (Subgrade_(top)) was defined as an independent
296 layer to assign the untreated subgrade, being Clay, and the three RG treated subgrades,
297 being CG10, CG20, and CG30. The remaining thickness of the subgrade (Subgrade_(bottom))
298 was defined as an infinite layer made of Clay.

299 The Mr value at a specific depth and location of the pavement or subgrade layers depends
300 on the stress state at that point. The stress state is governed by the wheel load, surcharge
301 from the above layers, and at-rest conditions. Therefore, to develop a realistic numerical
302 model, determining the Mr value under the loading conditions that apply to the specific
303 pavement profile using the predictive models is required. The determination of the Mr values
304 can be done through constitutive resilient modulus models, such as those presented in
305 Equations 3 and 4. In this regard, an iterative method was followed as recommended in the
306 Pavement Mechanistic-Empirical software manual [44]. In this iterative approach, the
307 following steps were followed:

308 1. An initial Mr value was assigned to the layer in question, and the analysis was run. For
309 this, the average of the Mr values obtained through the 15 loading sequences of the RLT
310 test was used as the initial Mr.

311 2. The vertical and horizontal components of the stress at the mid-depth (as recommended
312 by Huang [45]) of the ABC/subgrade layer of interest were extracted from FlexPAVE™ and
313 added to the surcharge generated by the above layers.

314 3. The predictive resilient modulus models were used to estimate the M_r corresponding to
1 315 the specific estimated stress state.

2
3 316 4. The estimated M_r was compared with the M_r initially assigned to the subgrade layer.

4
5 317 5. If the assumed and obtained M_r through steps 1 and 4 were more than 2%, the procedure
6 318 was repeated as the second iteration. The iterations continued until the assigned and
7 319 estimated M_r values converged.

3 Results and discussions

10 320
11
12 321 This section presents the experimental results, stress-strain response analysis by
13 322 incorporating the experimental results into the numerical model, and pavement performance
14 323 comparison analysis. First, RLT test data were obtained and were analyzed by fitting into the
15 324 two predictive resilient modulus models. Next, resilient modulus properties of Clay and the
16 325 three mixtures were assigned in the numerical model and the stress-strain response analysis
17 326 was carried out. Vertical and horizontal strains obtained through the response analysis were
18 327 next used for comparing the potential rutting and fatigue life of pavement systems
19 328 constructed on the four types of subgrades.

3.1 Resilient modulus test results

22 329
23
24 330 Compaction tests were carried out to determine the OMC and MDD of each sample for the
25 331 preparation of RLT specimens. Figure 4 shows the relationship between moisture content
26 332 and dry density of the four mixtures with MDD (t/m^3) and OMC (%) corresponding to each
27 333 compaction curve presented. Results show that increasing the RG content from 0% to 30%
28 334 results in a 22% decrease and a 9% increase in the OMC and MDD, respectively. Reduction
29 335 of the OMC could be attributed to the significantly lower water absorption potential of glass
30 336 particles compared to Clay [14], as well as greater MDD achieved in samples with higher RG
31 337 content which led to fewer available voids to be filled with water. Figure 4 also demonstrates
32 338 that the decreasing and increasing trends of OMC and MDD, respectively, for RG contents
33 339 up to 30% are approximately linear. This trend could potentially continue, although in a non-
34 340 linear form, until reaching the RG contents of 40% and 50%. After this, the mixture may
35 341 transition from a fine-graded blend, in which clay governs the behavior of the mixture, into a
36 342 coarse-graded blend according to the USCS classification scheme. It is expected that at RG
37 343 contents > 50%, with an increase in the RG content, the OMC and MDD slightly increase
38 344 and decrease, respectively. This trend was also observed and reported by Wartman, et al.
39 345 [24] who carried out compaction tests on clay-aggregate mixtures with coarse contents
40 346 between 0 and 100%. Investigating the compaction properties of clay-RG mixtures at RG
41 347 contents > 30% is recommended to be undertaken in future studies.

45 348 Figure 5 presents the M_r values obtained in each loading sequence presented in Table 1.
46 349 Solid lines in Figure 5 represent the average M_r value obtained through the 15 loading
47 350 sequences. The RLT test results showed that, in general, M_r values increased by increasing
48 351 the RG content. This can partially be attributed to the higher density (and hence lower void
49 352 ratio) of specimens with higher RG content. Higher density in one type of material has been
50 353 repeatedly reported to result in a greater resilient modulus [46, 47]. Another reason for the
51 354 increase in M_r of mixtures by the addition of RG is the increased percentage of particles with
52 355 rough surfaces. The greater roughness of particle surfaces in a specimen is known to yield
53 356 in the higher resilient modulus [48, 49]. By adding 10, 20, and 30% RG to the 11.8% existing
54 357 natural sand particles with relatively rough surfaces, the percentage of particles with a rough
55 358 surface in the mixture increased, leading to a greater resilient modulus. In general, the
56 359 resilient modulus is known to increase when the proportion of fines in a mixture decreases
57 360 [49].

361 The solid lines in Figure 5 show greater growth in Mr values by increasing the RG content
1 362 from 10% to 20% compared to other increments of RG. This is more clearly presented in the
2 363 last column of Table 3, which presents the average Mr values for the mixes and percentage
3 364 of increased Mr by adding RG. While the addition of 10% RG to Clay and CG20 results in a
4 365 26% and 15% increase in Mr, respectively, the increase of Mr by addition of 10% RG to
5 366 CG10 is 46%. This can be attributed to the fact that adding 20% RG to the Clay that
6 367 naturally contains close to 12% sand-size particles results in changing the classification of
7 368 the soil from "Clay" to "Sandy Clay" [50], and hence, a more significant increase in the Mr
8 369 values. The percentage of sand-size particles (natural sand + recycled glass) is presented in
9 370 the second column of Table 3, with CG20 containing more than 30% sand-size particles and
10 371 hence, classified as "sandy clay" [50].

13 372 Figure 6 schematically demonstrates the distribution of sand-size particles in the clay matrix
14 373 for CG10 and CG20. The increase in RG content together with the presence of natural sand
15 374 particles result in greater potential for coarse particle-on-particle interactions in CG20
16 375 compared to CG10. In CG10 specimens, the coarse particles are too distant to provide
17 376 particle-on-particle interactions, and hence the behavior of the mixture is dominantly
18 377 governed by the clay. With the increase in RG content, in addition to the greater possibility of
19 378 coarse particle interactions, there may be another factor that contributes to a more stable
20 379 force chain within the clay-aggregate mixture. The clay trapped between the sand-size
21 380 particles becomes stiffer during compaction and further loadings during RLT testing, and
22 381 forms bridge-like microstructures between the sand-size particles. This contributes to a
23 382 greater distribution of external loads within the mixture structure, and hence a more stable
24 383 force chain is offered as also discussed by Fei [51]. This results in a less compressible
25 384 specimen and consequently a greater resilient modulus.

29 385 Figure 7 illustrates plots of resilient modulus versus maximum axial stress (i.e. deviator
30 386 stress) for the mixtures studied in this research. Two points can be concluded from the
31 387 resilient modulus response of the mixtures under various combinations of axial and confining
32 388 pressures. Firstly, higher confining pressure results in a greater resilient modulus in each
33 389 specimen. Higher confinement can increase the inter-particle interlocking and internal friction
34 390 of the particles, and hence, less potential for strains, as explained by Nguyen and
35 391 Mohajerani [26] and Bhuvaneshwari, et al. [52]. With resilient modulus defined as the ratio of
36 392 cyclic axial stress to the recoverable strain, reduction of strain can result in greater Mr.
37 393 Secondly, the increases in axial stress, under the same confining pressure, result in greater
38 394 Mr. This can be due to the greater stress hardening of the specimens that occurred under
39 395 100 repetitions of a greater axial stress as explained by Puppala, et al. [53]. It should be
40 396 noted that several researchers such as Bhuvaneshwari, et al. [52] and Liu, et al. [47], among
41 397 others, have reported that the resilient modulus of untreated expansive soils was reduced
42 398 with an increase in axial stress due to stress softening; however, this contrasts the
43 399 experimental results on the Clay used in this research. This could be due to the presence of
44 400 more than 10% sand size particles in the natural untreated soil used in this research.

47 401 3.2 Data analysis using predictive models

50 402 The validity of the resilient modulus of the two-parameter and modified universal predictive
51 403 models was studied using the obtained RLT test datasets for all four mixtures. Plots of
52 404 Figure 8 compare the 60 measured and predicted Mr values. The higher visually evident
53 405 concentration of data points in the vicinity of the 1:1 line for the modified universal model
54 406 (Figure 8 (b)) shows that this model can provide a more accurate prediction.

56 407 Table 4 presents "k" coefficients of the two-parameter and modified universal models
57 408 achieved through regression analysis of the test results. The "k" coefficients depend on the
58 409 material type and physical properties of the material that is tested. Table 4 also shows the
60 410 coefficient of determination (R^2) and the result of the "goodness of fit" of each model for

each mixture following the Witczak, et al. [54] criteria. Witczak, et al. [54] have proposed a subjective criteria for the determination of the "goodness of fit", in which $R^2 \geq 90$, $0.70 \leq R^2 \leq 0.89$, $0.40 \leq R^2 \leq 0.69$, and $0.20 \leq R^2 \leq 0.39$, respectively, represent "Excellent", "Good", "Fair", and "Poor" fit. While the two-parameter model shows "Good" to "Excellent" fit with the experimentally obtained Mr values the modified universal model shows "Excellent" fit with results obtained for all four mixtures. Therefore, for the Mr analysis of the subgrade layers and further response analyses of this study, "k" coefficients obtained for the modified universal model were adopted. In this model, k_1 is proportional to the modulus of elasticity, hence, always a positive value; k_2 should be positive as an increase in bulk stress results in stress hardening of the specimen and accordingly, greater resilient modulus, and since the increase in octahedral shear stress results in stress softening and hence, lower resilient modulus, k_3 should be negative [46]. The k_1 , k_2 , and k_3 coefficients obtained using the modified universal model are positive, positive, and negative, respectively.

3.3 Stress-strain response of pavement systems

In order to determine the resilient moduli of the mixtures under loading conditions defined in the FlexPAVE™ model, the iterative approach explained in Section 2.3 was followed. In the first iteration, the average Mr values achieved through RLT testing, presented in Table 3, were assigned to the subgrade, and the model was run. In each iteration, the stresses at the mid-point of the 300 mm thick subgrade_(top) layer and those of another point located 150 mm below the subgrade_(top)-subgrade_(bottom) interface were extracted. Figures 9 (a) to 9 (c) show the distribution of the vertical stress (σ_z), transverse stress (σ_x), and longitudinal stress (σ_y), respectively, in the depth of pavement models with CG20 as subgrade_(top), as an example. The negative sign of σ_z indicates compressive stress, whereas the positive sign of σ_x and σ_y is an indication of tensile stresses.

Table 5 presents the final estimated values of Mr for each sample as well as the number of iterations carried out until less than 1% difference between assumed and estimated Mr was achieved. The resilient moduli presented in Table 5 were assigned to the subgrade layers of the pavement model, and the stress-strain response analysis was carried out.

Figure 10 compares the strain bulbs formed in two of the models, being the model with subgrade_(top) of Clay and that with subgrade_(top) of CG30. The distribution of the strains indicates overall lower strains in the depth of the pavement profile when the natural subgrade is mixed with RG. In particular, the reduction of horizontal strains (ϵ_x and ϵ_y) at the AC-ABC interface, and the reduction of vertical strain (ϵ_z) are observed in the plots.

The plots shown in Figure 11 demonstrate horizontal strains (transverse and longitudinal) at the surface course-base course interface (101.6 mm below the surface) and vertical strains at the base course-subgrade interface (254 mm below the surface) for all four mixtures. The tensile (horizontal) strain at the interface of the surface layer and the base layer generated due to the traffic loading is a major cause of the fatigue cracking and governs the fatigue life of pavements. The compressive (vertical) strain at the interface of the subgrade and aggregate base or subbase layer is known as rutting strain and controls the rutting life of pavements. Based on plots presented in Figure 11, greater RG content resulted in lower transverse (ϵ_x) and longitudinal (ϵ_y) strains that are of tensile nature and lower vertical strain (ϵ_z).

It is well known that the unbound granular layer (base or subbase) with a higher resilient modulus that overlays the softer subgrade layer controls the overall deformation at the subgrade level by spreading the stress [38]. Similarly, placing a RG-treated layer that is a stiffer layer, over a softer layer of untreated subgrade results in less vertical deformation at the subgrade level, and hence, less potential for rutting at the surface, as can be observed in the plots of Figure 10. The decreased magnitude of tensile strains at the AC-ABC interface

as a result of increased RG content can be attributed to the lower displacement of the pavement at this depth. Figure 12 (a) demonstrates the typical displacement behavior of flexible pavements under traffic loads, as well as the location of critical compressive vertical (ε_z) and tensile horizontal (ε_t) strains that govern the fatigue and rutting distresses, respectively. Figure 12 (b) compares the vertical displacement at the surface course-base course interface for models with clay subgrade and CG30 over clay subgrade. Considering the greater magnitude of the vertical deformation (D_z) in the pavement model founded on Clay compared to that founded on CG30, and accordingly, a greater sag induced in the surface layer, a higher tensile strain was expected at the bottom of asphalt concrete, as is the case presented in Figures 10 and 11.

3.4 Discussion on the pavement performance analysis

The main objective in pavement design is to provide sufficient thickness of structural layers for the service loads and ground conditions to resist structural distresses. The two major pavement distress types are fatigue cracking and rutting. While a major cause for rutting is the accumulation of vertical strains at the subgrade level, fatigue cracks occur due to the horizontal tensile strains at the bottom of the surface course. Equations 5 and 6 are widely used for the determination of fatigue (N_f) and rutting life (N_r) of pavements in terms of standard axle load repetitions, respectively [45].

$$N_f = f_1 \times \varepsilon_t^{-f_2} \times E^{-f_3} \quad (5)$$

$$N_r = f_4 \times \varepsilon_z^{-f_5} \quad (6)$$

In these equations, f_1 to f_5 are regression coefficients, ε_t and ε_z are the tensile (horizontal) and compressive (vertical) strains, respectively, and E is the average elastic modulus of the surface layer. The average elastic modulus of S9.5B surface layer for the vehicular speed of 80 km/h and the pavement temperature of 23°C is 4,224 MPa. Table 6 presents the f_1 to f_5 coefficients [45] proposed by two well-known organizations, being the Asphalt Institute, USA and the Transport and Road Research Laboratory, UK (Currently TRL).

It should be noted that values of N_r and N_f are not the real-life allowable number of repetitions, as coefficients f_1 to f_5 are proposed based on laboratory tests under conditions that may be different from the field [45]. The realistic allowable number of repetitions requires correction factors by comparing the field and laboratory conditions, which is out of the scope of this research. However, the obtained N_r and N_f values are sufficient for comparison purposes. The current research investigates whether the rutting and fatigue performance of pavements improves by stabilizing natural clay subgrades using RG. For the comparison analysis, the pavement model with clay subgrade was taken as the reference. The percentages of difference between N_f and N_r of other pavement models with those of the pavement system with clay subgrade were calculated and presented in Table 7.

Results presented in Table 7 show that the addition of even 10% of RG to Clay leads to 40 to 57% improved fatigue life and 22 to 25% improved rutting life. In general, the greater fine content in the mixture is known to result in a lower resilient modulus [49] and permanent deformation [55]. Therefore, introducing coarse particles (RG) in the clay matrix contributes to lower vertical and horizontal strains at the subgrade level and hence, an improved fatigue and rutting life of the pavement system. Another point obtained from Table 7 is the dramatic increase of fatigue life and rutting life by increasing the RG content from 10% to 20%. This is attributed to the fact that the addition of 20% sand-size particles to Clay samples results in the blend to transition from "Clay" classification to "Sandy Clay" classification and thus, a significant improvement of the subgrade mechanical characteristics. As illustrated in Figure 6, greater potential for coarse particle interaction, as well as the formation of clay micro-

508 bridge structures in CG20 compared to CG10 result in a more stable force chain within the
1 509 subgrade. This results in lower compressibility and hence, lower deformations, which results
2 510 in lower potential for rutting and fatigue distresses.

4 Conclusions

512 In this research, the improvement of the expansive clay subgrade properties using recycled
513 glass (RG) was investigated. First, density-moisture relationships and resilient modulus
514 responses of untreated Clay and Clay-RG mixtures were investigated. Next, using numerical
515 modeling techniques, the stress-strain response analysis of the pavement systems
516 constructed on the untreated subgrade and those founded on the RG-treated subgrade was
517 carried out. Using the outcomes of the response analysis, the rutting and fatigue
518 performance of the pavement systems on untreated and treated subgrades were compared.
519 The following conclusions were made based on the outcomes and analyses of this study.

- 520 • Increasing the RG content in the Clay-RG mixtures resulted in a greater maximum
521 dry density. The addition of 30% RG resulted in a 9% increase in maximum dry
522 density and a 22% reduction of the optimum moisture content required for field
523 compaction and preparation of the natural subgrade.
- 524 • The experimentally obtained resilient moduli of samples increased by increasing the
525 RG content in the mixtures.
- 526 • The most significant increment in the resilient modulus occurred when the RG
527 content was increased from 10% to 20%. This could be attributed to the transition of
528 "clay" soil, which naturally contained about 12% sand particles into a "sandy clay"
529 soil by adding 20% sand-size RG to the Clay.
- 530 • Increasing the RG content in the RG-treated subgrade layer led to a reduction of up
531 to 27% in compressive strains at the base course-subgrade interface and a reduction
532 of up to 75% in tensile strains at the bottom of the pavement surface layer.
- 533 • Decreased compressive and tensile strains by improving the clay subgrade using
534 recycled glass as mentioned above, resulted in increased fatigue life and rutting life
535 of the pavement structure.

536 In this research, a combination of experimental results and numerical analysis of the
537 pavement behavior revealed that the addition of recycled glass as a construction material
538 can significantly improve the behavior and performance of pavement subgrades. The
539 outcomes of this research aim to promote the application of sustainable construction
540 materials and methods as alternatives to the relatively costly and environmentally harmful
541 traditional approaches for the subgrade treatment. Highway designers and contractors
542 normally prefer the traditional construction approaches due to decades of experience with
543 traditional soil stabilizers. Resolving ambiguities and uncertainties of the performance of
544 non-traditional methods through rigorous experimental and analytical research works can
545 improve the construction industry's confidence in such sustainable approaches.

5 Acknowledgments

547 This work was supported by Victoria University through VU's Place-Based Planetary Health
548 fund [PH038].

6 References

549 [1] Y. Liu, C.-W. Chang, A. Namdar, Y. She, C.-H. Lin, X. Yuan, Q. Yang, Stabilization of
550 expansive soil using cementing material from rice husk ash and calcium carbide residue,
551 Construction and Building Materials 221 (2019) 1-11.
552

- 553 [2] J.R. Prusinski, S. Bhattacharja, Effectiveness of Portland cement and lime in stabilizing
1 554 clay soils, *Transp Res Record* 1652(1) (1999) 215-227.
2
- 3 555 [3] Z. Nalbantoğlu, Effectiveness of class C fly ash as an expansive soil stabilizer,
4 556 *Construction and Building Materials* 18(6) (2004) 377-381.
5
- 6 557 [4] N.-J. Jiang, Y.-J. Du, S.-Y. Liu, M.-L. Wei, S. Horpibulsuk, A. Arulrajah, Multi-scale
7 558 laboratory evaluation of the physical, mechanical, and microstructural properties of soft
8 559 highway subgrade soil stabilized with calcium carbide residue, *Can Geotech J* 53(3) (2015)
9 560 373-383.
10
- 11 561 [5] X. Kang, L. Ge, G.-C. Kang, C. Mathews, Laboratory investigation of the strength,
12 562 stiffness, and thermal conductivity of fly ash and lime kiln dust stabilised clay subgrade
13 563 materials, *Road materials and pavement design* 16(4) (2015) 928-945.
14 564
15
- 16 564 [6] A. Arulrajah, T.-A. Kua, C. Suksiripattanapong, S. Horpibulsuk, Stiffness and strength
17 565 properties of spent coffee grounds-recycled glass geopolymers, *Road Materials and*
18 566 *Pavement Design* 20(3) (2019) 623-638.
19
- 20 567 [7] M. Mirzababaei, A. Arulrajah, S. Horpibulsuk, A. Soltani, N. Khayat, Stabilization of soft
21 568 clay using short fibers and poly vinyl alcohol, *Geotextiles and Geomembranes* 46(5) (2018)
22 569 646-655.
23 570
24
- 25 570 [8] M.A. Rahgozar, M. Saberian, J. Li, Soil stabilization with non-conventional eco-friendly
26 571 agricultural waste materials: an experimental study, *Transportation Geotechnics* 14 (2018)
27 572 52-60.
28
- 29 573 [9] B. Mishra, M.K. Gupta, Use of randomly oriented polyethylene terephthalate (PET) fiber
30 574 in combination with fly ash in subgrade of flexible pavement, *Construction and Building*
31 575 *Materials* 190 (2018) 95-107.
32 576
33
- 34 576 [10] M. Mirzababaei, M. Miraftab, M. Mohamed, P. McMahon, Unconfined compression
35 577 strength of reinforced clays with carpet waste fibers, *Journal of Geotechnical and*
36 578 *Geoenvironmental Engineering* 139(3) (2013) 483-493.
37
- 38 579 [11] A. Soltani, A. Deng, A. Taheri, M. Mirzababaei, S.K. Vanapalli, Swell–shrink behavior of
39 580 rubberized expansive clays during alternate wetting and drying, *Minerals* 9(4) (2019) 224.
40
- 41 581 [12] A. Kumar, B.S. Walia, J. Mohan, Compressive strength of fiber reinforced highly
42 582 compressible clay, *Construction and Building Materials* 20(10) (2006) 1063-1068.
43 583
44
- 45 583 [13] E. Yaghoubi, A. Arulrajah, M. Yaghoubi, S. Horpibulsuk, Shear strength properties and
46 584 stress–strain behavior of waste foundry sand, *Construction and Building Materials* 249
47 585 (2020) 118761.
48
- 49 586 [14] M.M. Disfani, A. Arulrajah, M.W. Bo, R. Hankour, Recycled crushed glass in road work
50 587 applications, *Waste Management* 31(11) (2011) 2341-2351.
51
- 52 588 [15] M.M. Disfani, H.-H. Tsang, A. Arulrajah, E. Yaghoubi, Shear and Compression
53 589 Characteristics of Recycled Glass-Tire Mixtures, *Journal of Materials in Civil Engineering*
54 590 (2017) 06017003.
55 591
56
- 57 591 [16] M. Saberian, J. Li, D. Cameron, Effect of crushed glass on behavior of crushed recycled
58 592 pavement materials together with crumb rubber for making a clean green base and subbase,
59 593 *Journal of Materials in Civil Engineering* 31(7) (2019) 04019108.
60
61
62
63
64
65

594 [17] AGPT04E/09, Guide to pavement technology: part 4E: Recycled Materials, Austroads,
1 595 Sydney, Australia, 2009.
2

3 596 [18] MRWA-S-202, Sewerage Standards for Embedment, Melbourne Water Retail Agencies,
4 597 2015.
5

6 598 [19] J. Wartman, D.G. Grubb, A. Nasim, Select engineering characteristics of crushed glass,
7 599 Journal of Materials in Civil Engineering 16(6) (2004) 526-539.
8

9
10 600 [20] A. Arulrajah, E. Yaghoubi, M. Imteaz, S. Horpibulsuk, Recycled waste foundry sand as a
11 601 sustainable subgrade fill and pipe-bedding construction material: Engineering and
12 602 environmental evaluation, Sustainable Cities and Society 28 (2017) 343-349.
13

14 603 [21] EPA-Victoria, Solid industrial waste hazard categorisation and management
15 604 (IWRG631), Industrial waste resource guidelines (2009).
16

17 605 [22] U.S.EPA, National primary drinking water standards, EPA-F-94-001, Washington, D.C,
18 606 1999.
19

20
21 607 [23] A.O. Eberemu, J.E. Edeh, A. Gbolokun, The geotechnical properties of lateritic soil
22 608 treated with crushed glass cullet, Advanced Materials Research, Trans Tech Publ, 2013, pp.
23 609 21-28.
24

25 610 [24] J. Wartman, D.G. Grubb, P. Strenk, Engineering properties of crushed glass-soil blends,
26 611 Geotechnical engineering for transportation projects 2004, pp. 732-739.
27

28 612 [25] I. Ikara, A. Kundiri, A. Mohammed, Effects of waste glass (WG) on the strength
29 613 characteristics of cement stabilized expansive soil, American Journal of Engineering
30 614 Research (AJER) 4(11) (2015) 33-41.
31

32
33 615 [26] B. Nguyen, A. Mohajerani, Possible simplified method for the determination of the
34 616 resilient modulus of unbound granular materials, Road Materials and Pavement Design
35 617 (2016) 1-18.
36

37 618 [27] H.B. Seed, C.K. Chan, C.L. Monismith, Effects of repeated loading on the strength and
38 619 deformation of compacted clay, Highway research board proceedings, 1955.
39

40
41 620 [28] AASHTO, Mechanistic-Empirical Pavement Design Guide: A Manual of Practice,
42 621 Washington, DC, 2008.
43

44 622 [29] Y.D. Wang, B. Keshavarzi, Y.R. Kim, Fatigue performance prediction of asphalt
45 623 pavements with FlexPAVETM, the S-VECD model, and DR failure criterion, Transp Res
46 624 Record 2672(40) (2018) 217-227.
47

48 625 [30] A. Norouzi, D. Kim, Y.R. Kim, Numerical evaluation of pavement design parameters for
49 626 the fatigue cracking and rutting performance of asphalt pavements, Materials and Structures
50 627 49(9) (2016) 3619-3634.
51

52
53 628 [31] F.R. Padula, S. Nicodemos, J.C. Mendes, R. Willis, A. Taylor, Evaluation of fatigue
54 629 performance of high RAP-WMA mixtures, International Journal of Pavement Research and
55 630 Technology 12(4) (2019) 430-434.
56

57 631 [32] S.H. Cho, Evaluation of Interfacial Stress Distribution and Bond Strength between
58 632 Asphalt Pavement Layers, A thesis submitted in partial fulfillment of the requirements for the
59
60
61
62
63
64
65

633 Degree of Doctor of Philosophy in Civil Engineering, North Carolina State University,
1 634 Raleigh, NC, 2016.
2

3 635 [33] L.C. Chow, D. Mishra, E. Tutumluer, Aggregate base course material testing and rutting
4 636 model development, 2014, p. 116.
5

6 637 [34] AS-1289.7.1.1, Method 7.1.1: Soil reactivity tests—Determination of the shrinkage index
7 638 of a soil—Shrink-swell index, Standards Australia International, Sydney, NSW, 2003.
8

9
10 639 [35] S.G. Fityus, D.A. Cameron, P.F. Walsh, The shrink swell test, Geotech Test J 28(1)
11 640 (2005) 92-101.
12

13 641 [36] AS-2870, Residential slabs and footings, Standards Australia International, Sydney,
14 642 NSW, 2011.
15

16 643 [37] AASHTO-T307-99, Standard Method of Test for Determining the Resilient Modulus of
17 644 Soils and Aggregate Materials, American Association of State Highway and Transportation
18 645 Officials, Washington, DC, 2007.
19

20
21 646 [38] M.W. Frost, P.R. Fleming, C.D. Rogers, Cyclic triaxial tests on clay subgrades for
22 647 analytical pavement design, Journal of transportation Engineering 130(3) (2004) 378-386.
23

24 648 [39] ASTM-D698, Standard Test Methods for Laboratory Compaction Characteristics of Soil
25 649 Using Standard Effort (12 400 ft-lbf/ft³ (600 kN-m/m³)), ASTM International, West
26 650 Conshohocken, PA, 2012.
27

28 651 [40] R.G. Hicks, C.L. Monismith, Factors influencing the resilient response of granular
29 652 materials, Highway research record 345 (1971) 15-31.
30

31
32 653 [41] AASHTO, Guide for Design of New and Rehabilitated Pavement Structures, National
33 654 Cooperative Highway Research Program, American Association of State Highway and
34 655 Transportation Officials, Washington, D.C, 2002.
35

36 656 [42] AASHTO-T378, Standard Method of Test for Determining the Dynamic Modulus and
37 657 Flow Number for Asphalt Mixtures Using the Asphalt Mixture Performance Tester (AMPT),
38 658 American Association of State Highway and Transportation Officials, Washington, DC, 2017.
39

40
41 659 [43] TMR, Guideline for structural design procedure of pavements on lime stabilised
42 660 subgrades, Department of Transport and Main Roads The State of Queensland, Australia,
43 661 2020.
44

45 662 [44] L. Khazanovich, C. Celauro, B. Chadbourn, J. Zollars, S. Dai, Evaluation of subgrade
46 663 resilient modulus predictive model for use in mechanistic–empirical pavement design guide,
47 664 Transp Res Record 1947(1) (2006) 155-166.
48

49 665 [45] Y.H. Huang, Pavement analysis and design, PEARSON EDUCATION LIMITED, Upper
50 666 Saddle River, NJ, 2004.
51

52
53 667 [46] K. George, Prediction of resilient modulus from soil index properties, University of
54 668 Mississippi, 2004.
55

56 669 [47] X. Liu, X. Zhang, H. Wang, B. Jiang, Laboratory testing and analysis of dynamic and
57 670 static resilient modulus of subgrade soil under various influencing factors, Construction and
58 671 Building Materials 195 (2019) 178-186.
59
60
61
62
63
64
65

672 [48] R.D. Barksdale, S.Y. Itani, Influence of Aggregate Shape on Base Behavior, Transp Res
1 673 Record 1227 (1989) 173-182.
2
3 674 [49] F. Lekarp, U. Isacsson, A. Dawson, State of the Art. I: Resilient Response of Unbound
4 675 Aggregates, Journal of Transportation Engineering 126(1) (2000) 66-75.
5
6 676 [50] AS-1726, Geotechnical site investigations, Standards Australia Sydney, NSW, 2017, p.
7 677 72.
8
9
10 678 [51] K. Fei, Experimental study of the mechanical behavior of clay–aggregate mixtures,
11 679 Engineering Geology 210 (2016) 1-9.
12
13 680 [52] S. Bhuvaneshwari, R. Robinson, S. Gandhi, Resilient modulus of lime treated expansive
14 681 soil, Geotechnical and Geological Engineering 37(1) (2019) 305-315.
15
16 682 [53] A.J. Puppala, L.R. Hoyos, A.K. Potturi, Resilient Moduli Response of Moderately
17 683 Cement-Treated Reclaimed Asphalt Pavement Aggregates, Journal of Materials in Civil
18 684 Engineering 23(7) (2011) 990-998.
19
20
21 685 [54] M. Witczak, K. Kaloush, T. Pellinen, M. El-Basyouny, H. Von Quintus, NCHRP Report
22 686 465: Simple Performance Test for Superpave Mix Design, TRB, National Research Council,
23 687 Washington, D. C., 2002.
24
25 688 [55] F. Lekarp, U. Isacsson, A. Dawson, State of the art. II: Permanent strain response of
26 689 unbound aggregates, Journal of transportation engineering 126(1) (2000) 76-83.
27
28 690
29 691
30
31
32
33
34
35
36
37
38
39
40
41
42
43
44
45
46
47
48
49
50
51
52
53
54
55
56
57
58
59
60
61
62
63
64
65

692 **List of Tables:**

1
2
3
4
5
6
7
8
9
10
11
12
13
14
15
16
17
18
19
20
21
22
23
24
25
26
27
28
29
30
31
32
33
34
35
36
37
38
39
40
41
42
43
44
45
46
47
48
49
50
51
52
53
54
55
56
57
58
59
60
61
62
63
64
65

- 693 Table 1. Stress combinations in RLT test for subgrade soils as recommended by AASHTO-T307-99 [37]
- 694
- 695 Table 2. Prony coefficients for asphalt concrete
- 696 Table 3. Average values of Mr for each mix and percentage of increased Mr by adding RG
- 697 Table 4. The model k coefficients and evaluation of the "Goodness of Fit"
- 698 Table 5. Estimated Mr values used for modelling
- 699 Table 6. Regression coefficients used in this research (adopted from Huang [45])
- 700 Table 7. The percentage of difference in Nf and Nr of models with CG subgrades compared to the benchmark model with Clay subgrade
- 701

702
703

704 **List of Figures:**

- 1
2 705 Figure 1. Images of (a) dried lumps of clay, (b) the crusher, and (c) the soil grinder used for
3 706 preparation of dry clay
4
5 707 Figure 2. Properties of the clay and recycled glass used for the classification of the materials
6
7 708 Figure 3. The modeled pavement profile
8
9 709 Figure 4. Dry density vs. moisture relationships of the Clay and Clay-RG mixtures
10
11 710 Figure 5. The Mr values in each loading sequence
12
13 711 Figure 6. The schematic diagram comparing interactions between clay, RG and natural sand
14 712 particles in CG10 and CG20
15
16 713 Figure 7. Resilient modulus vs maximum axial stress plots for (a) Clay, (b) CG10, (c) CG20,
17 714 and (d) CG30.
18
19 715 Figure 8. Measured versus predicted Mr values using (a) the two-parameter model and (b)
20 716 the modified universal model.
21
22 717 Figure 9. Distribution of (a) vertical stress (σ_z), (b) transverse stress (σ_x) and (c) longitudinal
23 718 stress (σ_y) in the depth of pavement models with CG20 as subgrade(top)
24
25 719 Figure 10. Plots of (a) transverse, (b) longitudinal, and (c) vertical strain bulbs for Clay
26 720 subgrade and (d) transverse, (e) longitudinal, and (f) vertical strain bulbs for CG30 subgrade
27
28 721 Figure 11. Plots of (a) transverse strain and (b) longitudinal strain versus time at surface
29 722 course-base course interface, and (c) vertical strain versus time at base course-subgrade
30 723 interface
31
32 724 Figure 12. (a) Typical displacement behavior of flexible pavements under traffic loads and
33 725 (b) vertical displacement versus time at AC-ABC interface.
34
35
36
37
38
39
40
41
42
43
44
45
46
47
48
49
50
51
52
53
54
55
56
57
58
59
60
61
62
63
64
65

[Click here to view linked References](#)

Tables

Table 1. Stress combinations in RLT test for subgrade soils as recommended by AASHTO-T307-99 [37]

Sequence Number	0	1	2	3	4	5	6	7
Confining stress, σ_c (kPa)	41.4	41.4	41.4	41.4	41.4	41.4	27.6	27.6
Bulk stress, Θ (kPa)	151.9	138.0	151.9	165.5	179.5	193.2	96.5	110.4
Sequence Number	8	9	10	11	12	13	14	15
Confining stress, σ_c (kPa)	27.6	27.6	27.6	13.8	13.8	13.8	13.8	13.8
Bulk stress, Θ (kPa)	123.8	137.9	151.7	55.3	69.0	82.9	96.7	110

Table 2. Prony coefficients for asphalt concrete

ρ_i (s)	E_i (kPa)	ρ_i (s)	E_i (kPa)
2.00E+11	2,380	2.00E-01	3,173,760
2.00E+10	4,130	2.00E-02	3,761,120
2.00E+09	7,330	2.00E-03	3,104,720
2.00E+08	13,420	2.00E-04	2,497,320
2.00E+07	25,710	2.00E-05	1,851,650
2.00E+06	52,450	2.00E-06	1,323,710
2.00E+05	115,270	2.00E-07	917,490
2.00E+04	270,180	2.00E-08	624,310
2.00E+03	641,430	2.00E-09	419,320
2.00E+02	1,401,350	2.00E-10	279,300
2.00E+01	2,533,100	2.00E-11	185,000
2.00E+00	3,595,620	E_∞	60,490

Table 3. Average values of Mr for each mix and percentage of increased Mr by adding RG

Blend	Sand size particles (%)	Average Mr (MPa)	Mr increase compared to Clay (%)	Mr increase by adding 10% RG (%)
Clay	11.8	52.0	0	0
CG10	21.8	65.5	26	26
CG20	31.8	95.9	84	46
CG30	41.8	110.7	113	15

Table 4. The model k coefficients and evaluation of the "Goodness of Fit"

Model	Two-parameter model				Modified universal model			
Parameter	Clay	CG10	CG20	CG30	Clay	CG10	CG20	CG30
k_1	5.67	1.61	15.24	30.27	0.514	0.631	0.929	1.121
k_2	0.46	0.77	0.38	0.27	0.522	0.868	0.418	0.320
k_3	-	-	-	-	-0.529	-0.807	-0.298	-0.448
R^2	0.939	0.936	0.946	0.821	0.989	0.982	0.969	0.911
Goodness of fit	Excellent	Excellent	Excellent	Good	Excellent	Excellent	Excellent	Excellent

Table 5. Estimated Mr values used for modelling

Sample	Number of iterations	Estimated Mr for:	
		Subgrade _(top)	Subgrade _(bottom)
Clay	3	47.2	30.3
CG10	3	54.7	32.0
CG20	3	85.4	31.5
CG30	3	95.4	31.6

Table 6. Regression coefficients used in this research (adopted from Huang [45])

Organization	Proposed Regression Coefficients				
	f ₁	f ₂	f ₃	f ₄	f ₅
Asphalt Institute	0.0795	3.291	0.854	1.36E-09	4.48E+00
Transport and Road Research Laboratory	1.7E-10	4.32	0	6.18E-08	3.95E+00

Table 7. The percentage of difference in Nf and Nr of models with CG subgrades compared to the benchmark model with Clay subgrade

Criteria	Agency/Organization	Difference from Clay Subgrade (%)		
		CG10	CG20	CG30
Fatigue life (X direction)	Asphalt Institute	40	337	499
	Transport and Road Research Laboratory	55	593	949
	Average	47	465	724
Fatigue life (Y direction)	Asphalt Institute	41	357	534
	Transport and Road Research Laboratory	57	636	1028
	Average	49	497	781
Rutting life	Asphalt Institute	25	147	190
	Transport and Road Research Laboratory	22	122	156
	Average	23	135	173

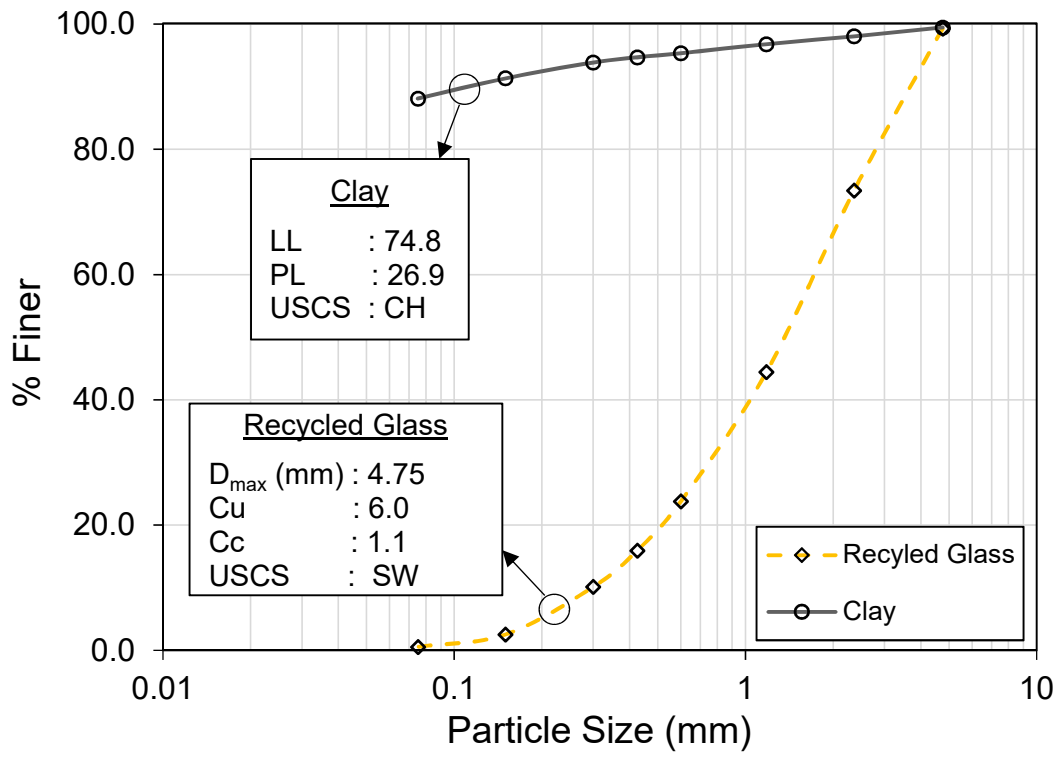
Figure 1

[Click here to access/download;Figure;Fig. 1- Clay_Preparation.pdf](#)

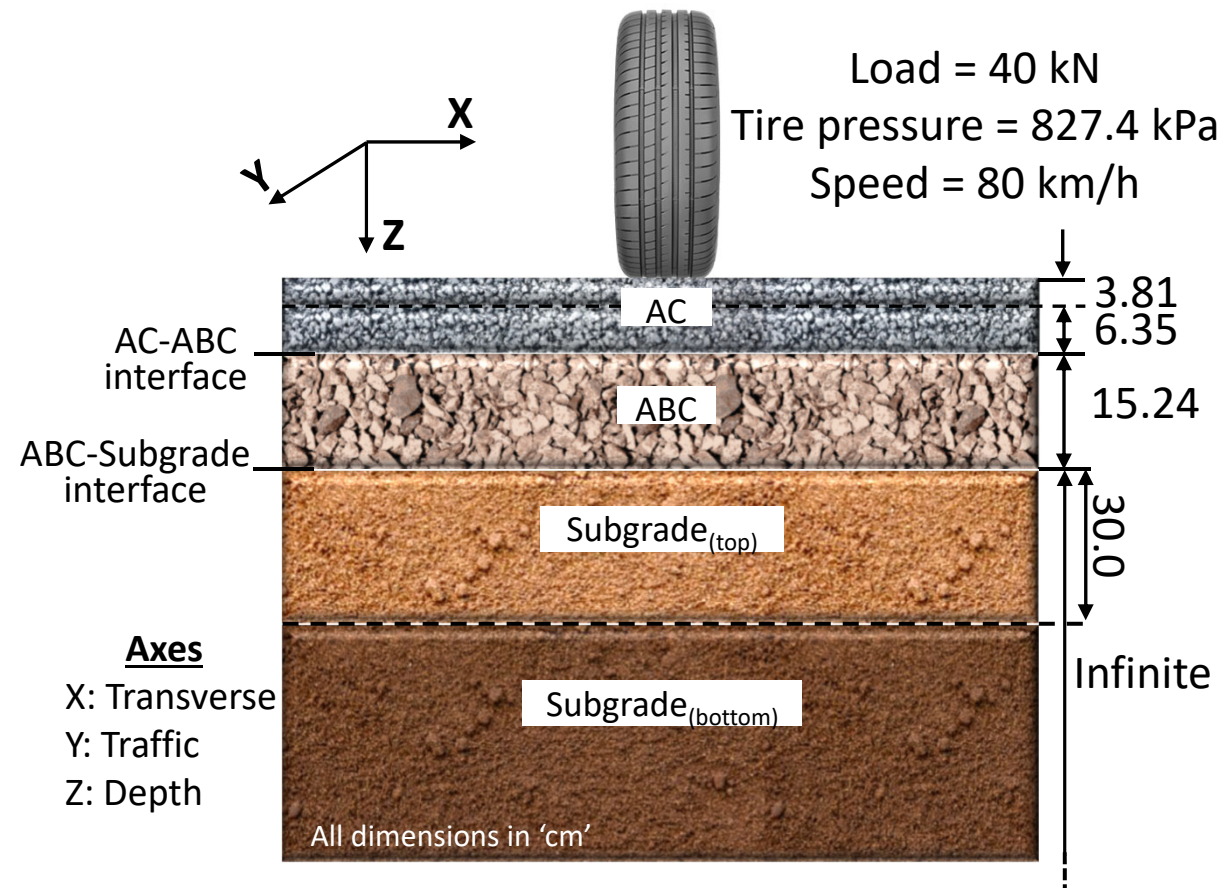
[Click here to view linked References](#)



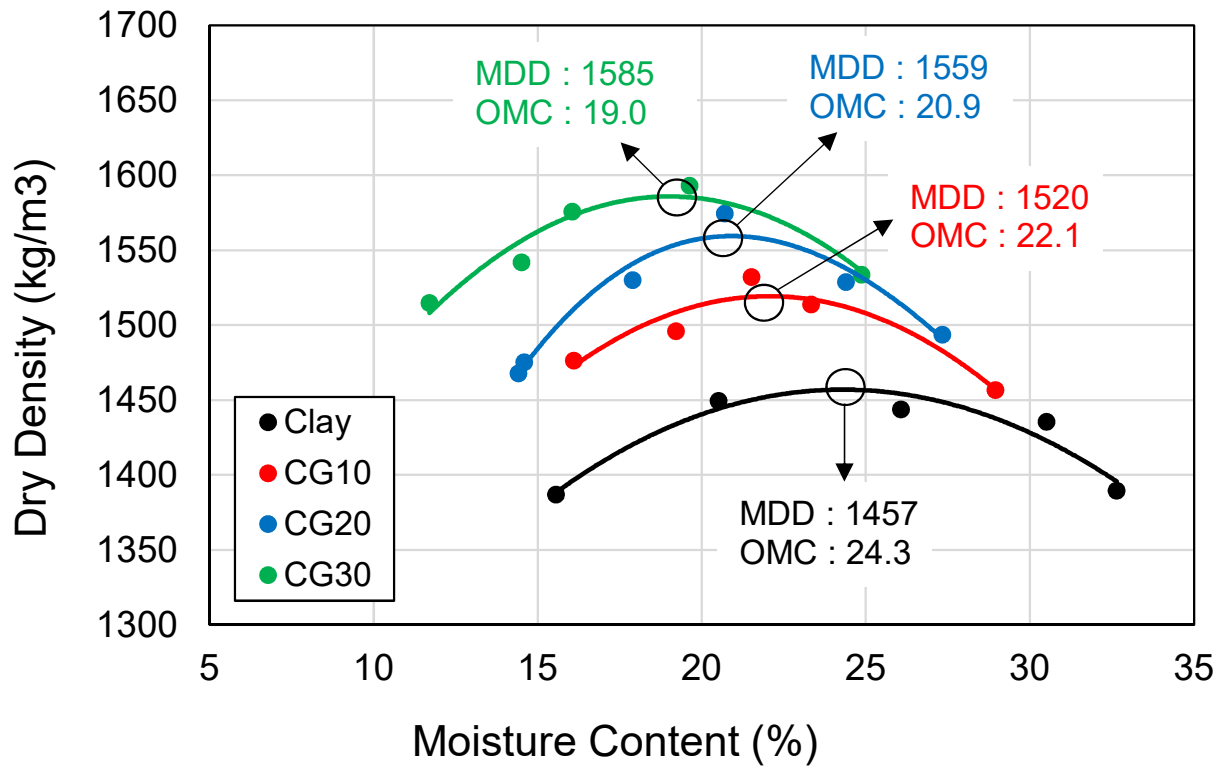
[Click here to view linked References](#)

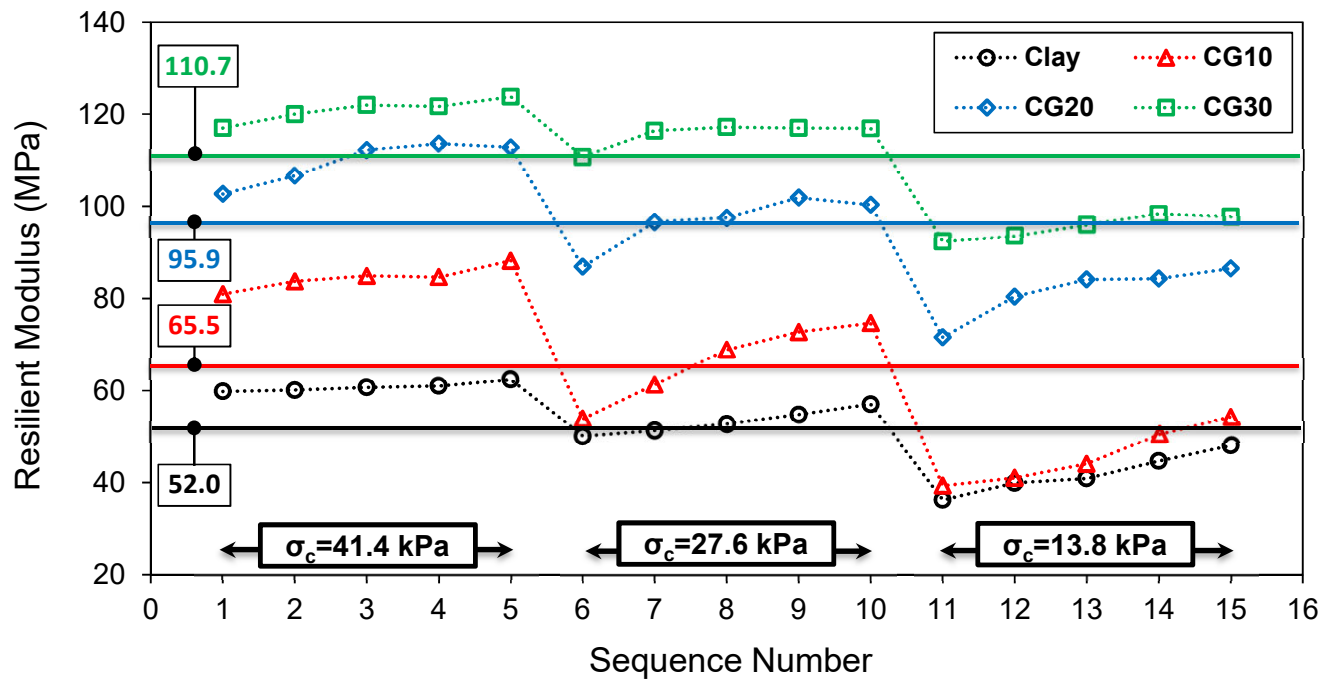


[Click here to view linked References](#)

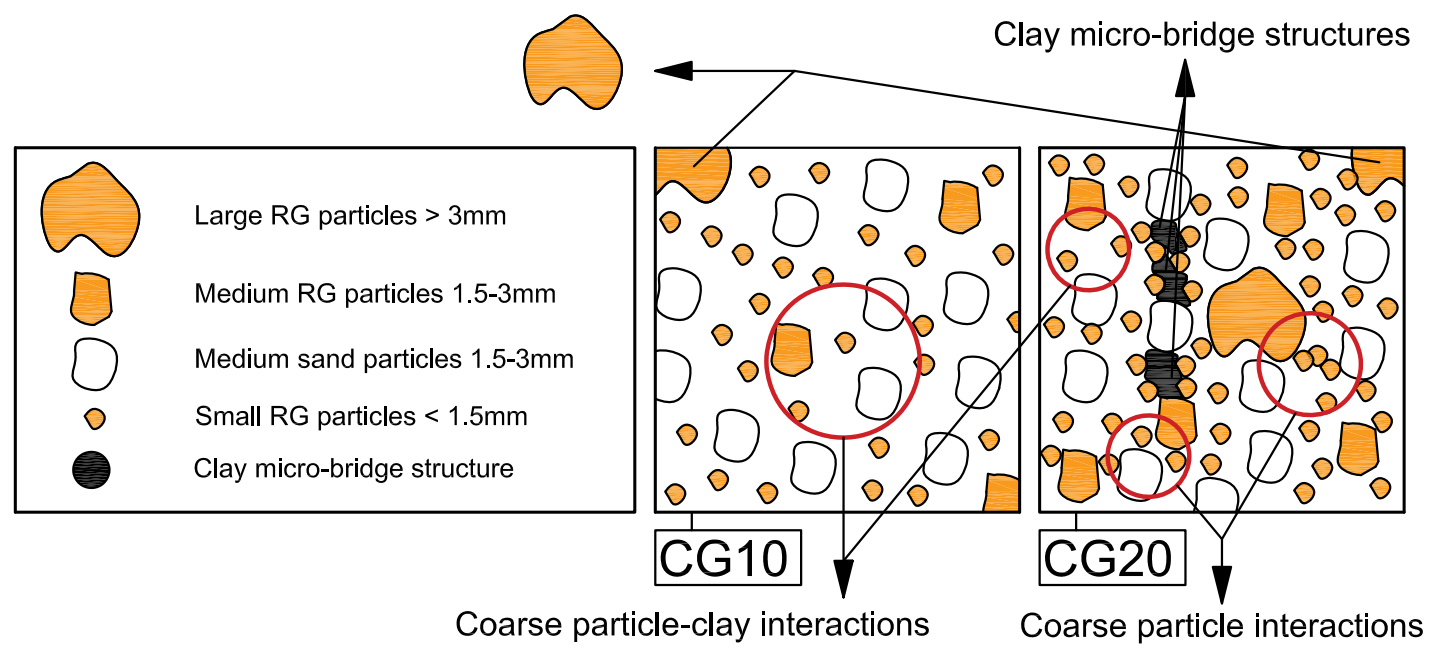


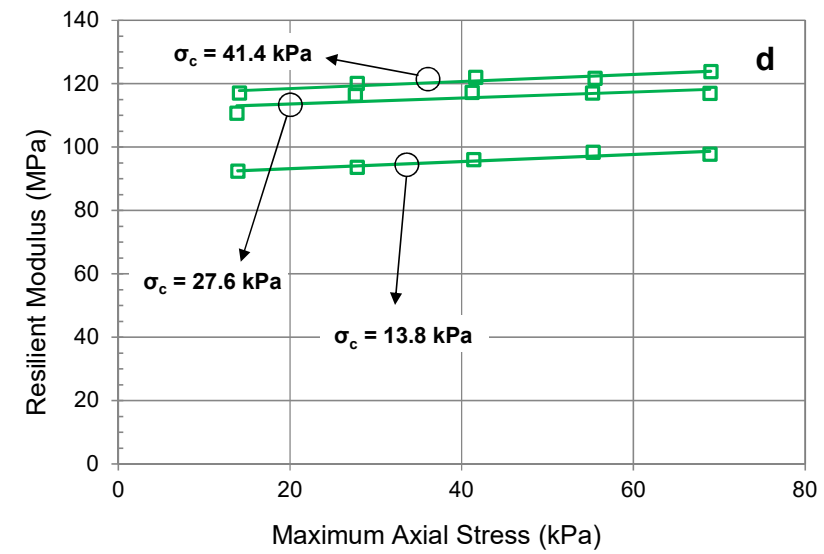
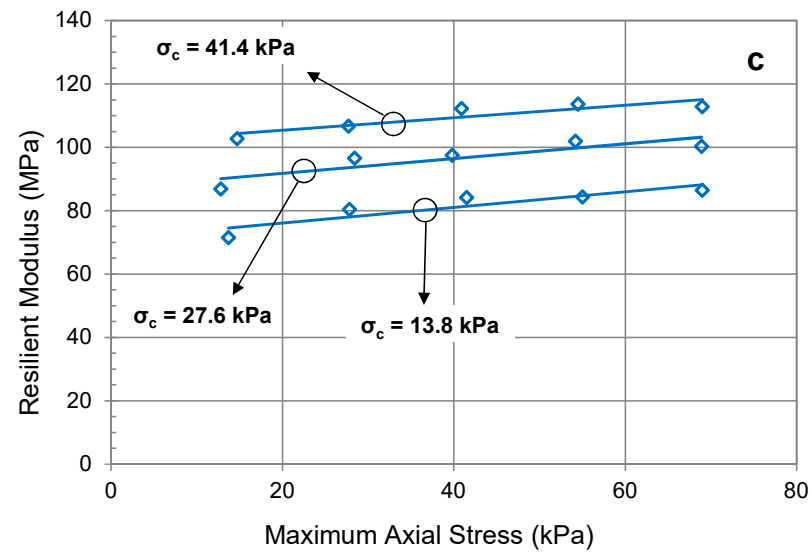
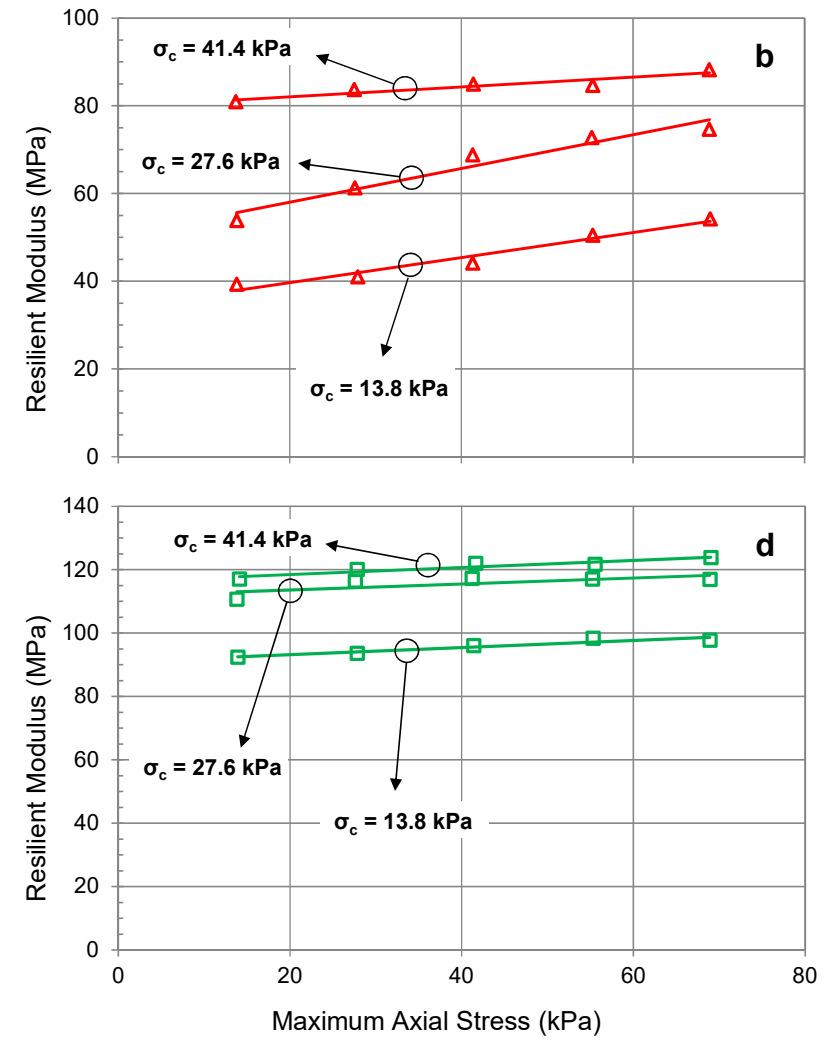
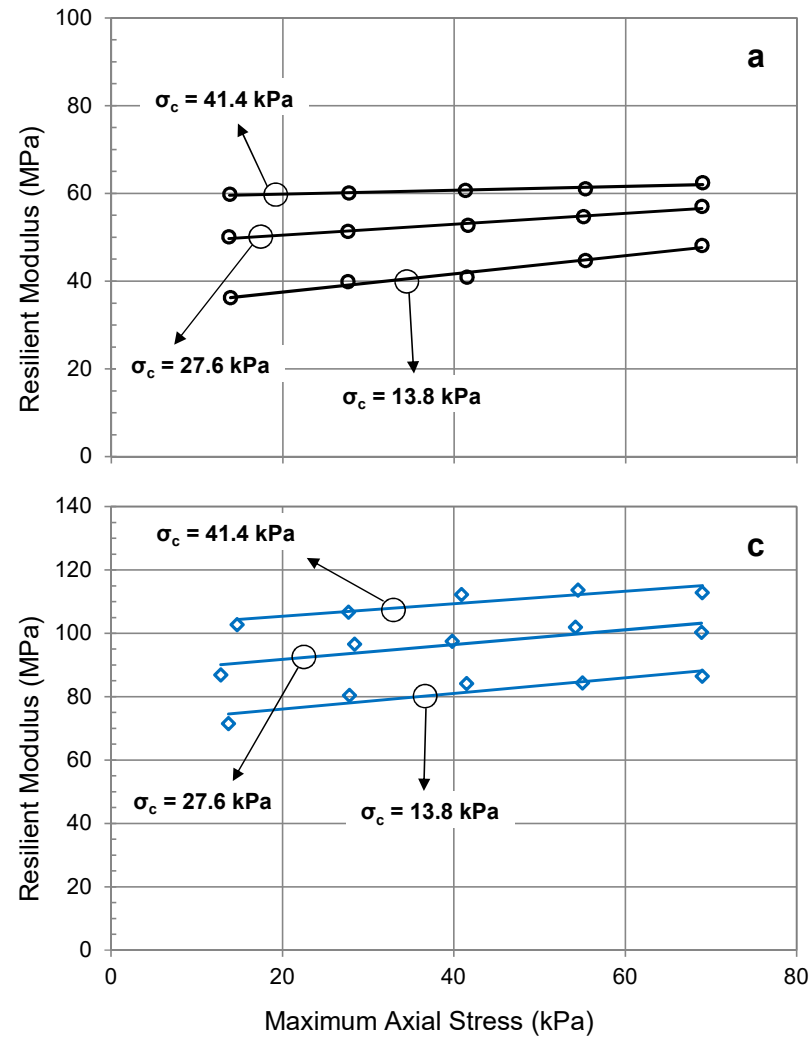
[Click here to view linked References](#)



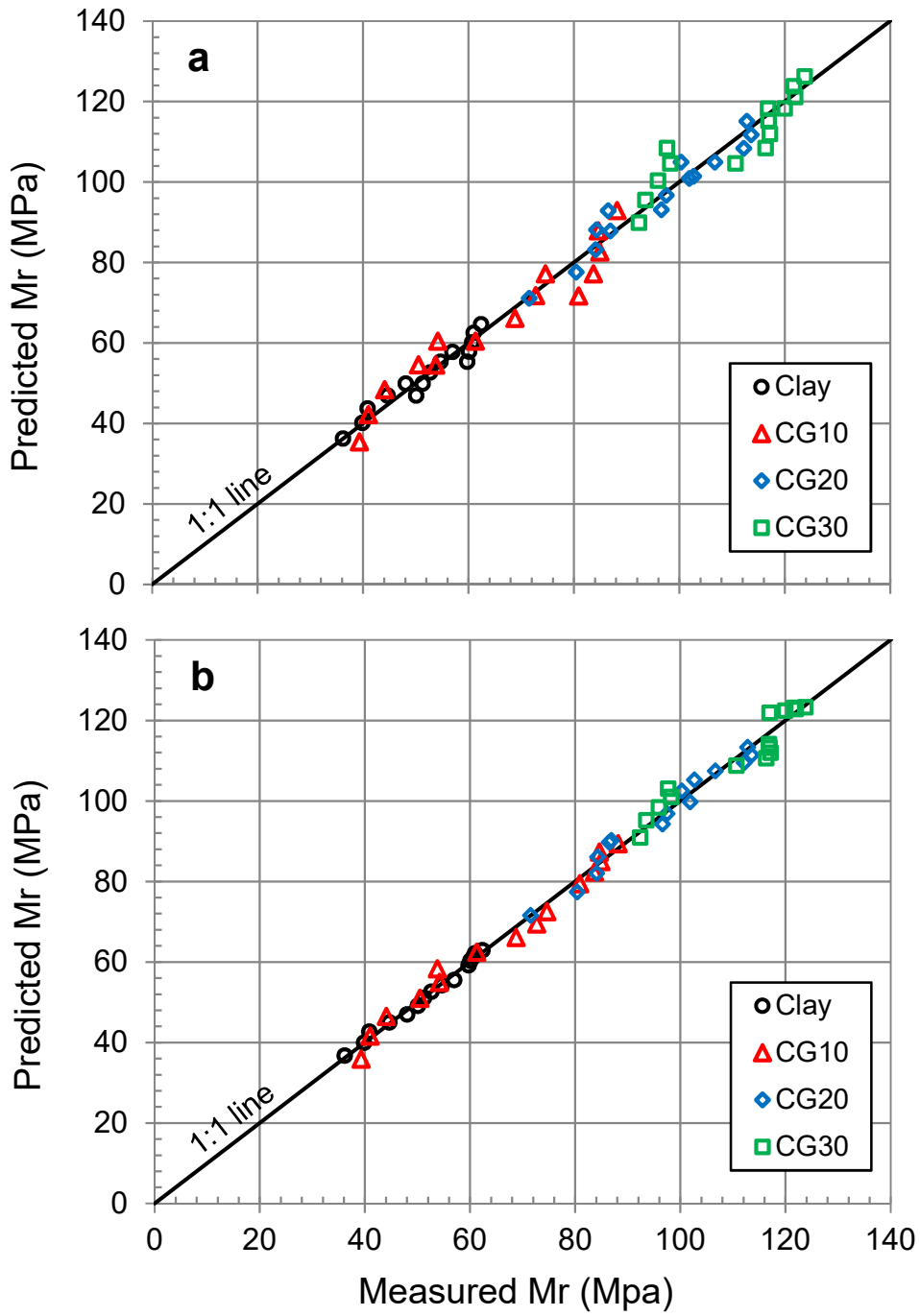
[Click here to view linked References](#)

[Click here to view linked References](#)



[Click here to view linked References](#)

[Click here to view linked References](#)



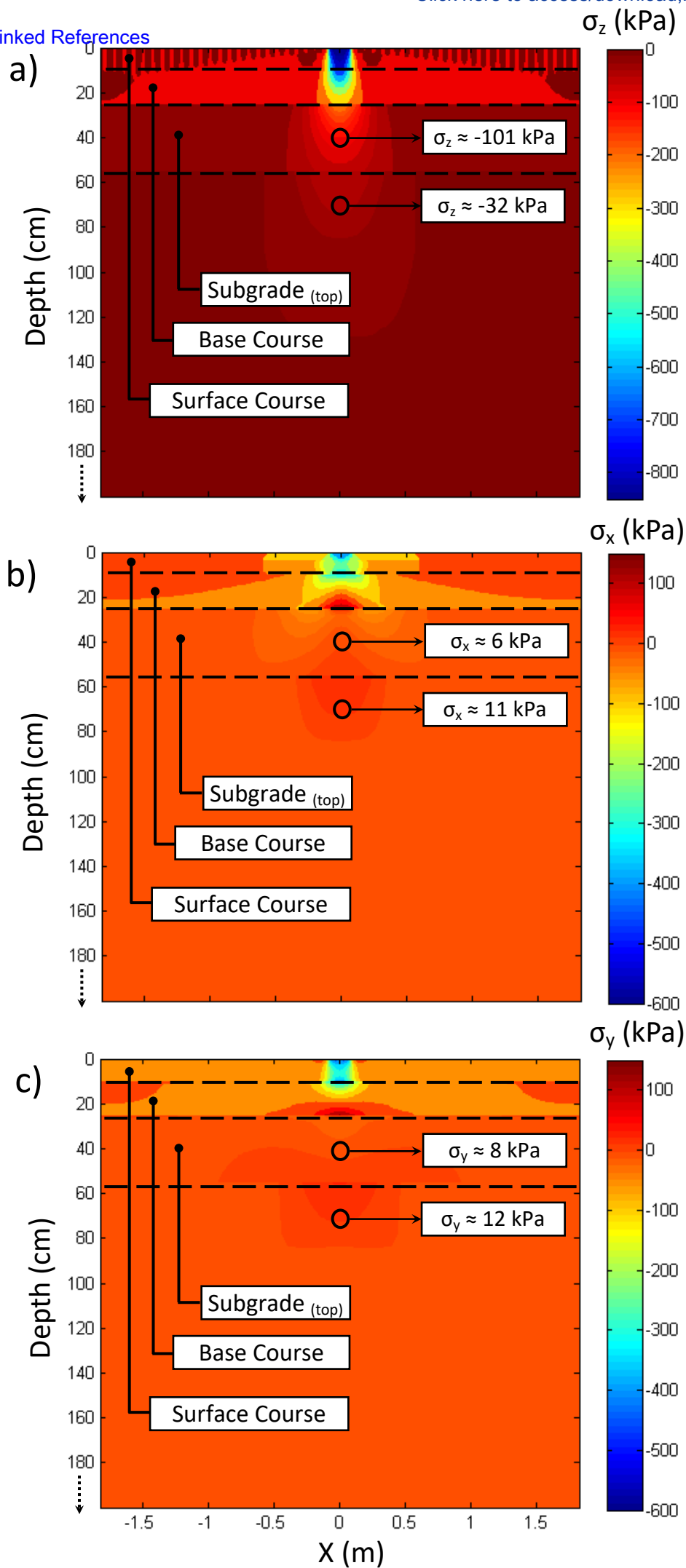
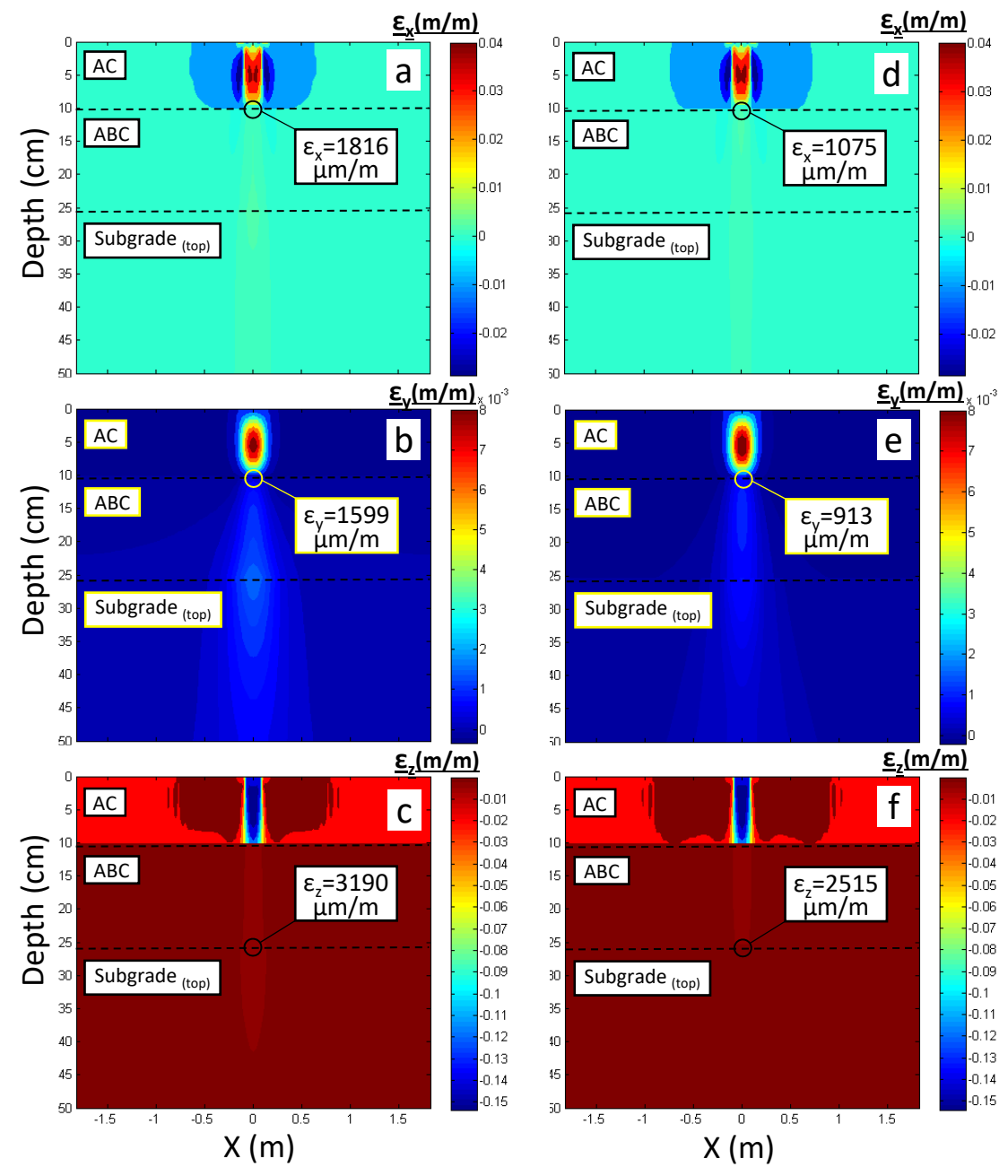
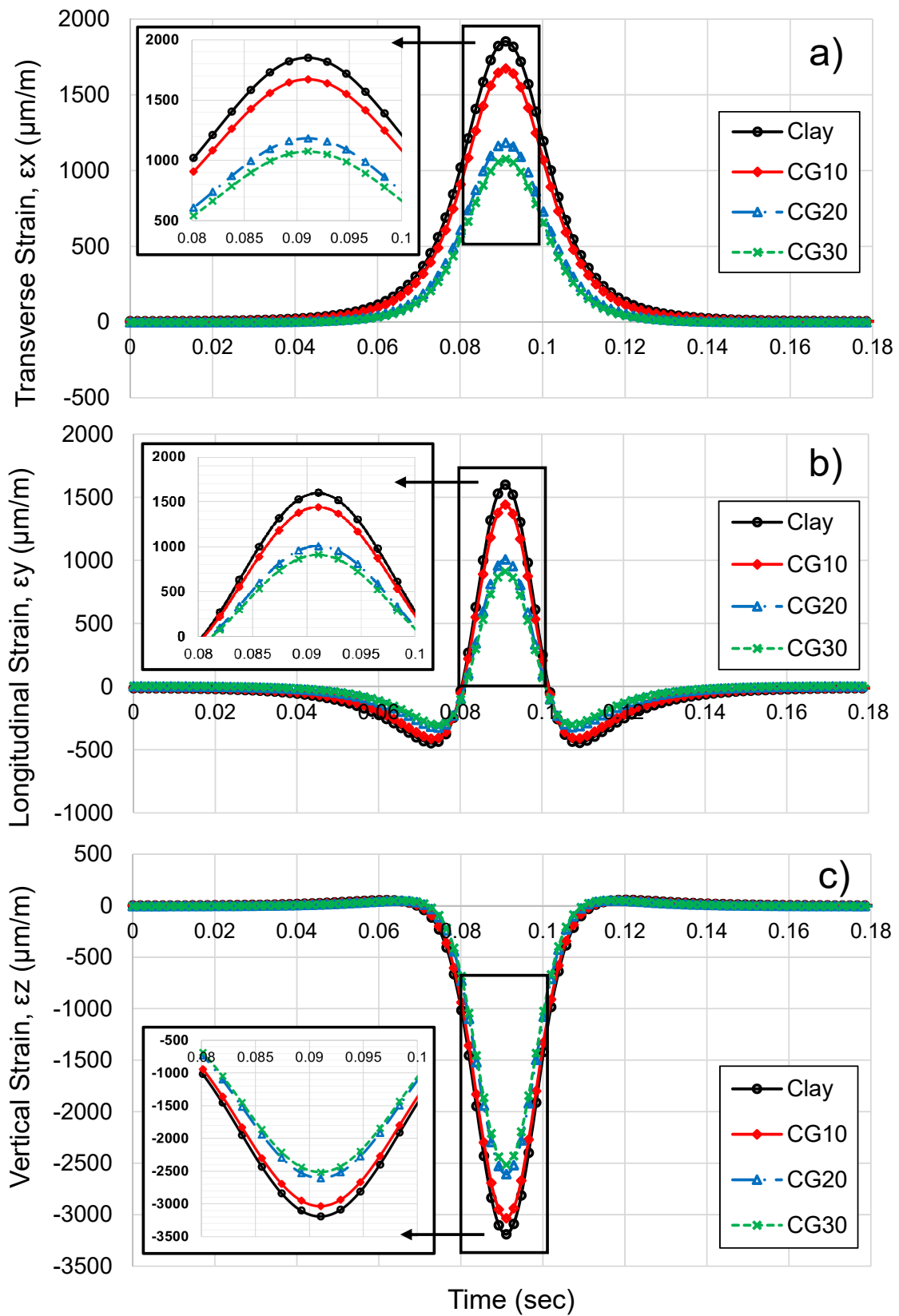
[Click here to view linked References](#)

Figure 10

[Click here to view linked References](#)



[Click here to view linked References](#)

[Click here to view linked References](#)